ISSN 0018-151X, High Temperature, 2018, Vol. 56, No. 1, pp. 109–123. © Pleiades Publishing, Ltd., 2018.
Original Russian Text © L.V. Bykov, A.M. Molchanov, D.S. Yanyshev, I.M. Platonov, 2018, published in Teplofizika Vysokikh Temperatur, 2018, Vol. 56, No. 1, pp. 104–120.

REVIEWS

Modern Approaches for Calculating Flow Parameters during a Laminar–Turbulent Transition in a Boundary Layer

L. V. Bykov*, A. M. Molchanov, D. S. Yanyshev***, and I. M. Platonov**

Moscow Aviation Institute (National Research University), Moscow, Russia

**e-mail: bykov@mai.ru*

***e-mail: alexmol_2010@mail.ru*

****e-mail: dyanishev@gmail.com*

Received June 20, 2016

Abstract—We analyze modern methods for calculating heat and hydrodynamic flow parameters in a boundary layer during the laminar–turbulent transition. The main approaches for describing the phenomenon of laminar–turbulent transition are examined. Each approach is analyzed. The manner in which different factors influence the laminar–turbulent transition is studied. An engineering model of the laminar–turbulent transition in a high-velocity flow is presented.

DOI: 10.1134/S0018151X18010042

CONTENTS

INTRODUCTION

The problem of hypersonic velocity is becoming increasingly important due to active development of the aviation and space industries. Engineers and scientists are making attempts to create a vehicle that operates at Mach numbers $M > 6$ at high altitudes with the required strength parameters. Flights with hypersonic velocities in dense atmospheric layers cause new problems, which must be solved. The shape of the vehicle should be characterized by a low drag coefficient with the necessary lift force, while the heat protection of the structure should absorb heat loads caused by high enthalpy of the incoming flow and by extreme heat fluxes. In many cases the extreme heat and mechanical loads that occur in structural elements of a high-velocity vehicle are caused by phenomena that occur in a boundary layer and in particular, by transition from laminar flow conditions into turbulent ones.

Main parameters defining vehicle performance such as frictional drag, heat fluxes at the surface of the vehicle, and lift force depend on the boundary-layer parameters.

The heat fluxes that act on the structural elements of the vehicle are most important at supersonic and hypersonic velocities (for example, for reusable spacecraft). The structure should be protected against high heat fluxes. Numerous experiments have shown that in a turbulent boundary layer the heat fluxes are higher by dozens of times than in a laminar layer. That is the reason that during the design of modern high-velocity vehicles it is very important to properly predict the place of the laminar–turbulent transition and to determine whether it is possible to affect it.

Proper prediction of the laminar–turbulent transition is also very important for investigating flows in channels. The problem has been studied properly for simple flow geometries (pipes with a simple cross section without turbulence stimulators and artificial roughness); while flows in channels with artificial roughness need further investigation [1].

The results of investigations (performed in Russia and abroad) on boundary-layer stability under different conditions are presented in this paper. Special

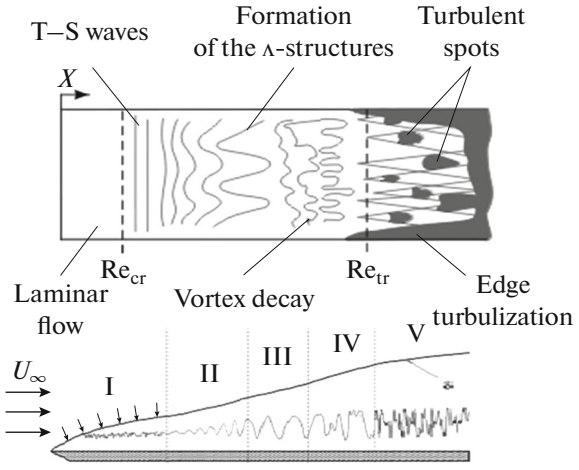

Fig. 1. A picture of the instabilities and turbulence development in a boundary layer.

attention is paid to the changes in flow conditions in the boundary layer, to the main factors that cause such changes, and to methods for predicting such phenomena.

This review contains data on both high-velocity and low-velocity flows, since the majority of methods for investigating the laminar–turbulent transition were developed initially for low-velocity flows (for an incompressible approximation).

1. THE MECHANISMS FOR TRANSITION TO TURBULENCE

The phenomenon of the laminar–turbulent transition has not been studied up to present. It is known that the main feature of turbulent flow is irregular pulsed variations in instantaneous parameters (such as velocity, temperature, and pressure).

A flow does not change from laminar to turbulent instantly. Separate ordered vortex structures occur in a flow, which disintegrate to smaller vortexes; finally, the layered ordered fluid flow is destroyed.

Figure 1 illustrates the modern conception of the laminar–turbulent transition (hereinafter the LT transition) in a medium with small initial disturbances at relatively low velocities of the incoming flow [2] (Re is the Reynolds number).

The first stage, stage I, of the examined process is called receptivity [3]. Disturbances in the incoming flow such as vortexes and sonic waves act on the boundary layer in the form of stable or unstable fluctuations. The form and intensity of these disturbances determine the initial conditions of the disturbances in the boundary layer (amplitude, frequency, and phase), which can cause the failure of the laminar boundary layer (due to the intensification process). The receptivity examines the initiation of instability waves, not their development.

In the receptivity area external disturbances are transformed into instability waves of the boundary layer.

The first mode of instability is waves in the form of viscous instability, which cause low-frequency vortex disturbances. For the case of a low-velocity flow the first mode is presented by Tollmien-Schlichting waves, which are most unstable in the form of 2D disturbances. For high velocities (for supersonic flows) 3D inclined waves of the first mode are the most unstable.

Disturbances of the second mode (the Mack mode) are intrinsic to compressible high-velocity ($M > 3$) boundary layers. Such instabilities cause high-frequency acoustic (not viscous) disturbances, which rise faster than T–S waves. The second mode is the dominant mechanism of the high-velocity flow transition if there are no strong transverse flows, Görtler vortexes, and bypass transition. In this case the specific conditions for dominating second-mode disturbances are determined by the flow conditions (in particular, by heat conditions at the wall). As an example, for a heat-insulating flat plate the second-mode disturbances are dominant at $M > 4$ according to the linear theory of stability [4].

The transverse flow becomes unstable if there is bending in the velocity profile. One example of such a flow is the 3D boundary layer at a sweptback wing. The nonlinear interactions are intrinsic to transverse disturbances. According to the theory, the traveling waves of a transverse flow increase faster than any other waves, but in practice transverse standing waves are studied since they are efficiently generated by roughness at a flow-around surface [5].

Görtler instability consists of longitudinal counter-rotating vortexes, which are common for Prandtl-Meyer flow in a boundary layer. They can occur both naturally, when the streamlines are curved, and artificially, after obstacles that are placed in the flow. The main instability that causes longitudinal counter-rotating vortexes is centrifugal instability, when the centrifugal force is higher than the radial pressure gradient [6].

Several different instabilities can occur simultaneously or separately. Which instability occurs depends on several factors, such as the incoming flow velocity, wall curvature, roughness, and irregularity. If oscillations in a boundary layer are small, the disintegration follows path *A* (Fig. 2) and the process of growth of disturbances can be described by the linear theory of stability. Such growth is not intensive; it occurs far from the initial segment and variations in the pressure gradient, temperature gradient and injection into the boundary layer from the surface can influence it.

The second stage, stage II, of the process is the linear growth of eigenmodes of instability waves in the boundary layer, which can occur in the form of eigen-

solutions of homogenous linearized equations for disturbances.

If the amplitude of the oscillations increase, 3D and nonlinear interactions in the form of secondary instabilities occur in the boundary layer. At this stage the waves propagate with the same phase velocity, which makes it possible to transfer energy from primary (basic) waves to secondary waves; as a result, the secondary waves grow rapidly.

In area III the mechanisms of secondary instability generate oblique waves by means of nonlinear interactions. In the area of tertiary instability IV layers connected with instantaneous bending in the velocity profile generate high-frequency fluctuations (oscillations, peaks, and striped structures) and turbulent spots. Turbulent spots are accumulated and associated; as a result a turbulent area forms (area V).

The amplitude of the initial disturbances increases from left to right. The primary disturbances can be too small for measurement and it is possible to estimate them only indirectly according to the parameters of the incipient instability.

Since it is possible to calculate the boundary layer behavior in the case of linear instability, very often it is thought that the process follows path *A* and only linear growth is examined. Such an assumption is true for the flows with small disturbances of the free flow and with extensive segments of linear growth with respect to nonlinear growth.

At times, the flow disturbances are so large that the turbulent mode occurs significantly earlier, skipping the stage of linear growth via the so-called bypass mechanism [7]. This corresponds to path *E*. It has been historically established that only two scenarios for transiting to turbulence: *A* and *E* are investigated. We have begun to better understand which path the process of laminar–turbulent transition follows only recently as a result of a large volume of scientific work.

The stage of unsteady growth occurs if the instability waves interact with each other.

Scientific investigations in this field have shown that at the respective initial conditions unsteady growth can cause high amplitudes of disturbances. Such initial conditions depend on the receptivity of the boundary layer. Depending on the amplitude the unsteady growth, it can cause the modulation of 2D waves (path *B*), disturb the initial state up to secondary (nonlinear) instabilities (*C*) and/or transition according to the bypass mechanism (*D*).

2. APPROACHES FOR DETERMINING THE BOUNDARY-LAYER STABILITY

Here, we investigate the main approaches for determining the conditions of the laminar–turbulent transition. For simplification we examine the flow of an incompressible fluid. High-velocity flows are examined in part 3.

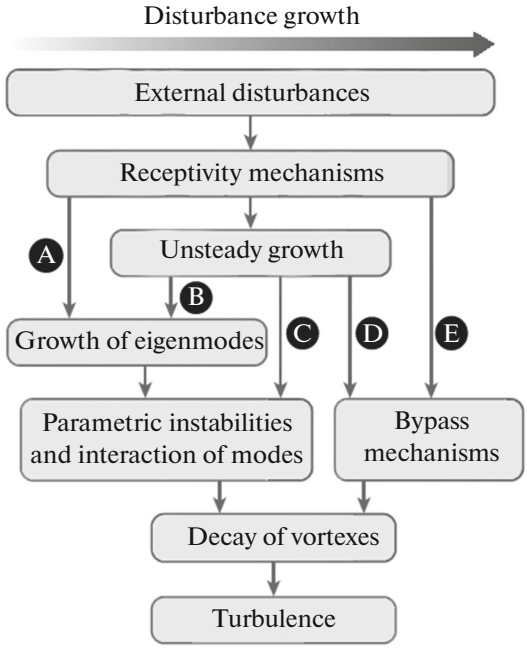

Fig. 2. A mechanism for transition to turbulence.

2.1. Stability-Theory Methods

For generating the laws of instability spreading in a boundary layer all physical values that characterize the flow conditions are presented in the form of two components: averaged and pulse components:

$$q = \overline{q}(\mathbf{x},t) + q'(\mathbf{x},t). \quad (1)$$

If we substitute values of the form (1) into Navier–Stokes equations we can obtain the precise equations for fluctuations. For an incompressible fluid these equations can be written as follows

$$\nabla \mathbf{u}' = 0, \quad (2)$$

$$\frac{\partial \mathbf{u}'}{\partial t} - \frac{1}{\mathrm{Re}}\nabla^2 \mathbf{u}' + (\mathbf{u}'\cdot\nabla)\overline{\mathbf{u}} + (\overline{\mathbf{u}}\cdot\nabla)\mathbf{u}' + \nabla p' = (\mathbf{u}'\cdot\nabla)\mathbf{u}'. \quad (3)$$

For small disturbances the right part of Eq. 3 can be accepted as equal to zero. In this case Eqs. (2), (3) are linear.

These equations are solved in the wave form (in the form of normal modes). For the parallel flow ($\overline{\mathbf{u}} = [u, 0, w]^T$) the solution is as follows:

$$\mathbf{q}' = \hat{\mathbf{q}}(y)\exp[i(\alpha x + \beta z - \omega t)], \quad (4)$$

where $\mathbf{q}' = [u', v', w', p']^T$ is the vector of the variables that describe the flow and $\hat{\mathbf{q}}(y) = [\hat{u}(y), \hat{v}(y), \hat{w}(y), \hat{p}(y)]^T$ is the vector of functions that describe the shape of the profile (amplitude) along the axis normal to the flow-around plane (axis *y*); α and β are the wave numbers;

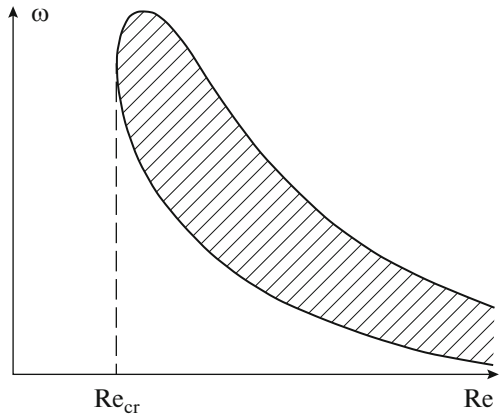

Fig. 3. The general form of a neutral curve.

ω is the frequency (in general case α, β, and ω are complex numbers).

From (4), it is seen that the disturbances grow infinitely, if $\mathrm{Im}(\alpha) < 0$, $\mathrm{Im}(\beta) < 0$, or $\mathrm{Im}(\omega) > 0$.

If there is a pronounced direction of flow (i.e., if the mean velocity of the flow is sufficiently high), all disturbances drift downstream and two types of flow instability occur.

If (in spite of the fact that disturbances drift downstream) at any fixed point in space for the smallest initial disturbances their amplitude rises infinitely with time, absolute instability occurs.

If the disturbances drift downstream so fast that at a fixed point in space for $t \to \infty$ the intensity of the disturbances goes to zero then convective instability occurs.

If we substitute (4) in the linearized set of equations (2), (3), we obtain the equation of the linear stability theory (LST)

$$L\hat{\mathbf{q}} = 0. \qquad (5)$$

The differential operator L includes derivatives only with respect to the y coordinate. If we apply different transformations to operator L, it becomes possible to obtain different forms of this set of equations, for example, a set of equations that consist of the Orr–Sommerfeld and Squire [8] equations (equations for the velocity disturbance and vorticity, respectively) or the Orr–Sommerfeld equation separately.

Usually LST equations are solved by determining the ω(Re) or α(Re) relationships (Fig. 3). The curve separating the crosshatched region is called the neutral curve. In this curve $\mathrm{Im}(\alpha) = 0$ or $\mathrm{Im}(\omega) = 0$. The crosshatched region is an area of instability and all of the other region is an area of stability (all disturbances in it die).

In the case of convective instability the disturbances increase only if the x coordinate increases downstream. In this case it is reasonable to formulate the problem as follows: it is necessary to determine the relationship between $\mathrm{Im}(\alpha)$ (and/or $\mathrm{Im}(\beta)$) and the disturbance frequency and the Reynolds number. For $\mathrm{Im}(\alpha) < 0$ unstable flow occurs, while for $\mathrm{Im}(\alpha) > 0$ the flow is stable. The boundary of the two areas is determined by the neutral curve, whose equation is as follows

$$\mathrm{Im}[\alpha(\omega, \mathrm{Re})] = 0.$$

Generalizing, it is possible to say that there are three main approaches to examining flow instability: a temporal theory that examines disturbances that increase with time (α and β are real and ω is complex); a spatial theory that examines the growth of disturbances in space (α and β are complex and ω is real), and a spatial and temporal theory (α, β and ω are complex numbers).

It is necessary to point out that in the general case the hypothesis on small disturbances is not correct.

In this case it may be impossible to solve equations (2), (3) since it requires large computational power (per se, the solution of equations (2), (3) is equivalent to direct numerical solution of the Navier–Stokes equations).

However, there is an intermediate solution: on the one hand it is not very sensitive to computation power, while on the other hand it is free of many disadvantages that are intrinsic to the linear theory.

This approach is called parabolized stability equations (PSE). The set of PSE equations makes it possible to calculate the behavior of disturbances both for parallel flows and for systems with complicated geometric configurations (for example, to calculate the flow around blades in impeller machines).

We do not present a statement of the method here, since there are many variants of its formulation. The parabolized equations of stability were examined in detail in [8].

LST and PSE describe the behavior of instability waves in a flow, but they do not determine the transition point.

At present, the semi-empirical e^N-method is used for determining when laminar flow transforms into turbulent flow.

It is accepted that transition to turbulence occurs when the amplitude of the instability wave increases by e^N times with respect to the initial amplitude at the neutral point (the first point, where $\mathrm{Im}(\alpha) = 0$).

It is possible to show that for the boundary layer at a flat plate

$$N = \ln\left(\frac{A_{\mathrm{tr}}}{A_0}\right) = -2\int_{R_0}^{R} \mathrm{Im}(\alpha)\, dR,$$

where $R = \sqrt{\mathrm{Re}_x} = \sqrt{\dfrac{\rho u x}{\mu}}$.

According to the empirical data the turbulence occurs at $N = 7–9$ [8].

This method has a disadvantage: it cannot be applied for all of the examined mechanisms of destruction of a laminar flow. In particular, it is impossible to predict laminar–turbulent transition via the bypass mechanism with its use.

Intensification conditions or conditions for the decrease of spontaneous small-amplitude instability waves are examined using the methods of the stability theory described above. The process of amplitude growth of spontaneous instability waves is a natural mechanism for the laminar–turbulent transition. As mentioned above, it occurs only if the level of external-flow turbulence is low.

In practice, the level of turbulence of the external flow is large and the stability theory approaches described above cannot be used directly. Mathematically, this is due to the fact that in the stability theory the growth of the disturbances is examined in an asymptotic approximation passing from the problem of initial and boundary conditions to the problem of searching for eigenvalues [9, 10].

We examine the flow in terms of the stability theory; we do not examine the dynamics of the system, we estimate the ability of the system to continue the infinite growth of disturbances.

However, in the general case such a problem definition is not very correct mathematically when we speak about a system described by Navier–Stokes equations (due to the properties of the operators of this system). This can occur as follows: a certain external disturbance that should decrease to zero as $t \to \infty$ (according to asymptotic analysis of the system) in reality increases greatly at a specific moment of time causing a transition to turbulence.

In other words, there are cases where a flow in which external disturbances should die out with time (according to stability theory) can transit to turbulence due to unsteady growth of a certain disturbance.

In the general case, the concept of unsteady growth means local development of a disturbance in contrast to the stability theory, where the possibility of disturbance development separating cases of its exponential growth or decrease within a certain range is examined.

For mathematical illustration let us write set (5) in the form of the Orr–Sommerfeld and Squire equations

$$\begin{bmatrix} L & 0 \\ C & S \end{bmatrix} \begin{bmatrix} \hat{u} \\ \hat{\Omega} \end{bmatrix} = 0, \tag{6}$$

where $\hat{\Omega}$ is the vorticity of the velocity disturbance, $L = S\Delta - i\alpha\dfrac{d^2\bar{u}}{dy^2}$ is the Orr–Sommerfeld operator, $S = -i\omega + i\alpha\bar{u} - \dfrac{\Delta}{\mathrm{Re}}$ is the Squire operator, $C = i\beta\dfrac{d\bar{u}}{dy}$ is the conjugation operator, and $\Delta = \dfrac{d^2}{dy^2} - \left(\alpha^2 + \beta^2\right)$ is the Laplace operator.

For $\beta = 0$ the equations of set (6) are independent. Their eigenmodes are Orr–Sommerfeld modes (for 2D definition of Tollmien–Schlichting waves) and Squire modes. Orr–Sommerfeld modes are solutions of Orr–Sommerfeld equations (equations for velocity disturbance) and of Squire equations (equations for vorticity disturbance), while Squire modes are solutions of Squire equations for $\hat{u} = 0$ or $\beta = 0$.

In all cases where $\beta \neq 0$ operator $C \neq 0$, i.e., the operator of the Navier–Stokes set of equations is not conjugated. This means that Orr–Sommerfeld modes and Squire modes can interact with each other under conditions of a non-flat flow. It is possible to show that for the case where Orr–Sommerfeld modes and Squire modes decrease individually, their unstationary interaction can cause significant growth of disturbance amplitude and it can cause the laminar–turbulent transition.

Usually, the concept of an intensification factor (a growth factor) is used for analyzing unsteady growth

$$G = \frac{E}{E_0}, \tag{7}$$

where E is the energy norm, which is determined differently for different flow types; the 0 index is the initial value.

As an example, for an incompressible flow this norm is an integral with respect to the kinetic energy of the disturbance

$$E = \int_0^\infty \left(u'^2 + v'^2 + w'^2\right)dy.$$

To analyze unsteady growth one determines the so-called optimal disturbances for which the intensification factor (7) is maximal. This makes it possible to determine the upper boundary of the intensification of disturbances in a flow and to understand which type of disturbance is the most likely to grow in a specific type of flow.

Very often unsteady growth is connected with a laminar–turbulent transition caused by surface roughness. However, there is no unified theory of the laminar–turbulent transition caused by roughness or by its separate elements.

2.2. Engineering Methods

The methods described above, in which equations for instability waves are used, are in good agreement with the experimental data; however, it is difficult to use them for solving engineering problems for different reasons.

First, it is necessary to be well trained in mathematics to use the methods of stability theory correctly.

Second, it is difficult to use these methods for flows with complicated geometric configurations.

Third, due to the characteristics of the described methods, it is very problematic to use them in modern CFD software.

From the practical point of view, approaches for determining the stability of laminar flow based on numerical simulation, such as direct numerical simulation, Langtry–Menter methods, and $k-k_L$- transition models, are more suitable.

Reynolds averaged Navier-Stokes equations (for compressible flows—Favre averaged) play the central role in the modern methods for calculating turbulent flows.

These equations are the basis of modern applied software such as Ansys CFX, Ansys Fluent, Star-CD, FlowVision, and LOGOS.

If the turbulent fluctuations go to zero, these equations transform into ordinary Navier–Stokes equations.

For such transformation it is convenient to introduce the intermittency factor [11] between the laminar flow model ($q \to \overline{q}$) and the model of turbulent flow ($q = \overline{q} + q'$)

$$\gamma = \frac{\tau_t}{\tau_L + \tau_t},$$

where τ_L, τ_t are the times within which the flow at a given point is in the laminar and turbulent states, respectively.

By using the intermittency factor and the Boussinesq hypothesis for turbulent stresses, it is possible to determine the mean viscosity coefficient μ_{eff} at a given flow point

$$\mu_{\text{eff}} = \mu + (1-\gamma)\mu_{nt} + \gamma\mu_T, \qquad (8)$$

where the index T indicates the turbulent flow, while nt is related to non-turbulent disturbances (transitive).

Alternately, it may be possible to impose a respective restriction to the turbulence source in the transport equation for the kinetic energy of the turbulence (which effects the viscosity coefficient).

The main disadvantage of this approach is that it is impossible to derive the respective equation for γ with the appropriate physical strictness.

It is only possible to assume that such an equation should have the standard form of the transport equation with a special source component:

$$\frac{\partial}{\partial t}(\rho\gamma) + \frac{\partial}{\partial x_j}(\rho\overline{u}_j\gamma) = \frac{\partial}{\partial x_j}\left[\left(\mu + \frac{\mu_T}{\sigma_\gamma}\right)\frac{\partial\gamma}{\partial x_j}\right] + \mathrm{F}_\gamma,$$

where σ_γ is the Prandtl–Schmidt number for the intermittency factor.

The boundary conditions recommended by Menter are as follows: on the wall $\frac{\partial\gamma}{\partial n} = 0$ (n is the normal to the wall surface); at the input $\gamma = 1$.

The input condition is chosen mainly according to numerical stability [12]. Its physical sense can be given by examining the bypass mechanism for transition to turbulence when the disturbances in the boundary layer are introduced from the external flow.

Let us point out that the intermittency factor is the "indicator" of flow conditions (it is equal to zero in laminar flow and to unity in turbulent flow); it does not regulate the turbulence level in the flow. As an example, if we use the value of the kinetic energy of the turbulence $k \to 0$ as a boundary condition, the turbulence level in the external flow also goes to zero in spite of the set value $\gamma = 1$.

The form of the source component F_γ depends on the model version (Menter et al. suggested several modifications (see, for example, [13, 14]). This practically determines the model behavior.

It is evident that it is most convenient to determine the source type by using the generalized experimental data on the laminar–turbulent transition as a function of local variables. Jointly with the chosen form of transport equation for γ, it removes the necessity to determine the concrete type of instability that causes transition.

The main problem is as follows: the majority of the experimental data on the laminar–turbulent transition are obtained in the form of relationships for integral quantities, in particular, for the Reynolds number $\mathrm{Re}_{\theta t}$, under which transition to turbulent flow occurs and which depends on the turbulence level in the external flow Tu, pressure gradient parameter, etc.:

$$\mathrm{Re}_{\theta t} = \frac{\rho U_\infty \theta_t}{\mu} = f\left(Tu\ldots\right)_\infty,$$

where θ_t is the thickness of the impulse loss in the boundary layer at which the flow mode changes (it is the integral performance of the boundary layer and cannot be determined at a point), $Tu = \left(\sqrt{2/3\,k}/u\right)\times 100\%$.

Menter and Langtry suggested a method for solving this problem.

Instead of the integral Reynolds number Re_θ it is suggested to use the so-called vortex Reynolds number Re_v, which is calculated using only the local parameters of the flow:

$$\mathrm{Re}_v = \frac{\rho y^2 S}{\mu}.$$

Here, y is the distance from the wall, $S = \sqrt{S_{ij}S_{ij}}$ is the invariant of the strain rate tensor

$S_{ij} = 1/2\left(\partial u_i/\partial x_j + \partial u_j/\partial x_i\right)$ (in several works $\Omega = \sqrt{\Omega_{ij}\Omega_{ij}}$ the invariant of the vorticity tensor $\Omega_{ij} = 1/2\left(\partial u_i/\partial x_j - \partial u_j/\partial x_i\right)$ is used).

The number Re_v has a maximum that is proportional to Re_θ approximately in the middle of the laminar boundary layer.

In [15] it was shown that for a laminar boundary layer without a pressure gradient

$$\mathrm{Re}_\theta = \frac{\mathrm{Re}_{v\max}}{2.193}.$$

It was also proven that for calculating the laminar–turbulent transition this relationship can be used without alteration, as well as for the cases of more complicated flows.

Here, Re_θ is replaced by the local Re_v. Moreover, $\mathrm{Re}_{\theta t}$ is a function of the integral parameters of the external flow (such as Tu_∞).

Here, it is necessary to introduce the local analog of $\mathrm{Re}_{\theta t}$. For this purpose in [12, 14, 15] a certain modified local Reynolds number $\widetilde{\mathrm{Re}}_{\theta t}$ for which the transport equation is derived artificially was introduced:

$$\frac{\partial}{\partial t}\left(\rho\widetilde{\mathrm{Re}}_{\theta t}\right) + \frac{\partial}{\partial x_j}\left(\rho\bar{u}_j\widetilde{\mathrm{Re}}_{\theta t}\right) = \frac{\partial}{\partial x_j}\left[\sigma_{\theta t}(\mu + \mu_T)\frac{\partial\widetilde{\mathrm{Re}}_{\theta t}}{\partial x_j}\right] + \mathrm{P}_{\theta t}.$$

According to [16], the empirical relationship between $\widetilde{\mathrm{Re}}_{\theta t}$ and the integral critical Reynolds number is obtained via numerical experiments:

$$\mathrm{Re}_{\theta c} = \begin{cases} \sum_{n=0}^{4} A_n\widetilde{\mathrm{Re}}_{\theta t}^{\,n}, & \widetilde{\mathrm{Re}}_{\theta t} \le 1870, \\ 0.518\widetilde{\mathrm{Re}}_{\theta t} + 308.23, & \widetilde{\mathrm{Re}}_{\theta t} > 1870, \end{cases}$$

where $A = \begin{pmatrix} -396.035\times10^{-2} \\ 101.207\times10^{-2} \\ -868.230\times10^{-6} \\ 696.506\times10^{-9} \\ -174.105\times10^{-12} \end{pmatrix}$.

According to [16] the model is not suitable for highly compressible flows.

The Menter–Langtry approach described above can be characterized as a pure phenomenological approach based on experimental data.

Another approach, which is an attempt to examine processes that occur in the laminar–turbulent transition in terms of the transport of disturbance energy, was described in [17].

The main idea is to present the energy of fluctuation k_{TOT} in the flow by two components

$$k_{\mathrm{TOT}} = k_L + k_T,$$

where k_L is the kinetic energy non-turbulent fluctuations ("laminar" energy) and k_T is the kinetic energy of the turbulence.

It is clear that non-turbulent fluctuations are of a large scale while the turbulent ones are of a small scale. The transport factor for non-turbulent fluctuations is the molecular viscosity, while for turbulent fluctuations it is the molecular and turbulent viscosities.

The model consists of three equations: for k_L, k_T, and the vortex dissipation rate ω.

$$\frac{D(\rho k_T)}{Dt} = \rho\left(P_{k_T} + R_{\mathrm{BP}} + R_{\mathrm{NAT}} - \omega k_T - D_T\right) + \frac{\partial}{\theta x_j}\left[\left(\mu + \frac{\rho\alpha_T}{\sigma_k}\right)\frac{\partial k_T}{\theta x_j}\right],$$

$$\frac{D(\rho k_L)}{Dt} = \rho\left(P_{k_L} - R_{\mathrm{BP}} - R_{\mathrm{NAT}} - D_L\right) + \frac{\partial}{\theta x_j}\left[\mu\frac{\partial k_L}{\partial x_j}\right],$$

$$\frac{D(\rho\omega)}{Dt} = C_{\omega 1}\frac{\rho\omega}{k_T}P_{k_T} + \left(\frac{C_{\omega R}}{f_W} - 1\right)\frac{\rho\omega}{k_T}(R_{\mathrm{BP}} + R_{\mathrm{NAT}}) - C_{\omega 2}\rho\omega^2 + C_\omega J_\omega\alpha_T f_W^2\frac{\rho\sqrt{k_T}}{d^3} + \frac{\partial}{\partial x_j}\left[\left(\mu + \frac{\rho\alpha_T}{\sigma_\omega}\right)\frac{\partial\omega}{\partial x_j}\right].$$

This model is in good agreement with the experimental results. The issue of whether it is possible to calculate the supersonic flows was not examined in [17].

3. THE LAMINAR–TURBULENT TRANSITION AT HIGH VELOCITIES

Flows at high velocities are characterized by some peculiarities that complicate the picture of the laminar–turbulent transition.

1. At velocities with M > 0.3 the compressibility is important. In particular, it becomes more difficult to generate the equations of the stability theory (see, for example, [18]).

2. During the transonic transition and during a further velocity increase, the wave structure of the flow changes greatly; the character of the laminar–turbulent transition also changes, respectively.

3. If the flow velocity increases, its energy also increases and it can affect the molecular structure and thermodynamic properties of the flow. Here, in the vicinity of boundary layer for certain Mach numbers of the external flow it is impossible to consider the gas as the ideal one. Moreover, under certain conditions it is impossible to characterize the gas by sole temperature.

As a result of all of these issues the problem of determining gas flow stability at high velocities becomes more complicated.

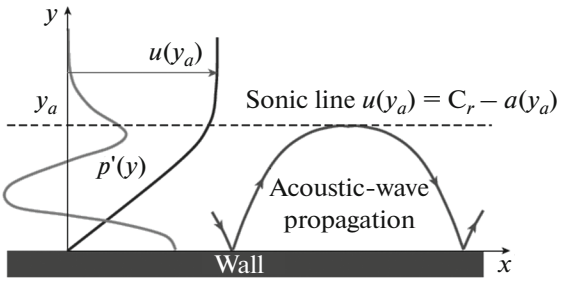

Fig. 4. Acoustic waves in a boundary layer [19].

At the present time only the theoretical approaches for solving the problem have been developed. These are based on stability theory and on the model of chemically nonequilibrium high-enthalpy flow. Universal applied methods have not been developed as yet in this field.

The main peculiarity of high-velocity flows with respect to incompressible flows in terms of their stability is a collection of persisting instability modes; these were classified for the first time by Mack [4].

Let us note that in the incompressible fluid examined above, the natural mechanism of laminar–turbulent transition is determined by Tollmien-Schlichting waves of a viscous nature.

In the case of compressible fluid flow with a sufficiently high velocity ($M > 3$) nonviscous disturbances (Mack modes) of an acoustic nature begin to develop in the flow.

Based on the example of an equation for nonviscous pressure disturbances, Mack showed that the occurrence of acoustic disturbances that did not die out in a flow is determined by the velocity of the disturbance phase with respect to the flow velocity and the sound velocity of the external flow.

According to this, the respective Mach number can be written as follows

$$\tilde{M} = \frac{u_e - c_r}{a_e},$$

where the index e is the external boundary of the boundary layer.

If $\tilde{M} > 1$, an area is formed in the flow where the mean velocity of the flow with respect to the phase velocity of of disturbances is higher than the sound velocity. The line (surface) that limits this area is called the sonic line. If this line (surface) exists, acoustic waves reflect from it and become trapped inside (Fig. 4). Here, u is the velocity profile, c_r is the phase velocity of disturbances, and p' is the profile of the pressure disturbances. Such trapped acoustic waves form Mack modes.

The amplitude of Mack modes increases more rapidly than the disturbance amplitude of the first mode. Due to this, the Mack modes are prevalent in the mechanism of the natural laminar–turbulent transition in the high-velocity flow for $\tilde{M} > 1$.

The behavior of Mack modes has been examined in detail by solving stability-theory equations written for compressible flow (in the linear and parabolic definitions) and experimentally. As an example, it has been found that the Mack modes are stabilized by the body front edge bluntness [20], and destabilized by wall cooling [21].

The problem of the variation of the chemical and thermal properties of a gas at hypersonic velocities (first of all due to reactions of dissociation and recombination) requires detailed investigation.

It is known that in a hypersonic flow intensive physical and chemical processes are connected with the excitation of a molecule's internal degrees of freedom, dissociation, chemical reactions between gas components, and the ionization of an atom.

Here, the set of equations for gas flow in the case of hypersonic flow should be combined with equations that describe these physical and chemical processes. Let us present the set of gas dynamic equations for a hypersonic air flow.

—The equation of continuity

$$\frac{\partial \rho}{\partial t} + \frac{\partial}{\partial x_j}(\rho u_j) = 0,$$

where ρ is the gas mixture density and u_j is the velocity component in the jth direction.

—The momentum equation

$$\frac{\partial}{\partial t}(\rho u_i) + \frac{\partial}{\partial x_j}(\rho u_j u_i + \delta_{ji} p - \tau_{ij}) = 0,$$

where p is the pressure and τ_{ij} is the tensor of viscous tensions.

—The equation of the total energy

$$\frac{\partial}{\partial t}(\rho E) + \frac{\partial}{\partial x_j}\left[\rho u_j\left(E + \frac{p}{\rho}\right) + q_{\mathrm{tr},j} + q_{\mathrm{v},j} + \sum_s V_{s,j}\rho_s h_s - u_i \tau_{ij}\right] = -Q_R.$$

Here, E is the total energy per mass unit; h_s specific (per mass unit) enthalpy; s is the bottom index that show the membership to component s; ρ_s is the density; $V_{s,j}$ is the diffusion velocity in the jth direction; $q_{\mathrm{v},j}$ is the density of heat flux of vibrational energy in the jth direction; $q_{\mathrm{tr},j}$ is the density of the heat flux of the tranlsational and rotational energy in the jth direction; and Q_R is the losses via radiation W/(m^3).

—The equation of the vibrational energy of the mth vibration mode

$$\frac{\partial}{\partial t}(E_{v,m}) + \frac{\partial}{\partial x_j}(E_{v,m}u_j + q_{v,m,j} + E_{v,m}V_{m,j}) = S_{v,m},$$
$$m = 1, 2, \ldots, N_M,$$

where $E_{v,m}$ is the specific (per volume unit) vibrational energy of the mth vibration mode; $q_{v,m,j}$ is the density of the heat flux of the vibrational energy of the mth vibration mode in the jth direction; $S_{v,m}$ is the source of vibrational energy caused by the V–T, V–V energy transition, the generation rate of the vibrational energy due to chemical reactions, as well as by the vibrational energy loss due to spontaneous deactivation of radiation; and N_M is the number of modes of the vibrational energy.

Here, $V_{m,j}$ is the diffusion velocity of the component to which the mth vibration mode is related.

A detailed discussion of the problem of how to calculate the radiation parameters was presented in [22, 23].

—The equation of mass conservation for a chemical component s

$$\frac{\partial}{\partial t}(\rho C_s) + \frac{\partial}{\partial x_j}(\rho C_s u_j + \rho C_s V_{s,j}) = \dot{w}_s,$$
$$s = 1, 2, \ldots, N_C - 1,$$

where $C_s = \rho_s/\rho$ is the mass fraction, $\dot{w}_s$ is the generation rate for s due to chemical reactions, and N_C is the number of components in the gas mixture.

The following assumptions are used in this set:

(1) the rotational energy modes are in equilibrium with the translational ones and they are determined by one translational-rotational temperature $T = T_{\text{tr}}$;

(2) the energy for exciting the electron states of a molecule is negligibly small with respect to other energy modes;

(3) it is accepted that the heat losses for radiation in the energy equations are caused mainly by deactivation of the vibrational modes;

(4) electron-to-ion energy transitions are not taken into account.

The gas mixture pressure p is described by Dalton's law and is equal to the sum of the partial pressures for the components p_s

$$p = \sum_{s=1}^{Nc} p_s = \sum_{s=1}^{Nc} \rho_s \frac{R_U}{M_s} T_{\text{tr}},$$

where R_U is the universal gas constant and M_s is the molecular mass.

The total energy E consists of the translational, rotational, vibrational, kinetic energy, and energy of chemical components

$$\rho E = \sum_{s=1}^{Nc} \rho_s C_{V\text{tr},s} T_{\text{tr}} + \sum_{m=1}^{N_M} E_{v,m} + \frac{1}{2}\rho u_i u_i + \sum_s \rho_s h_s^0,$$

where h_s^0 is the heat of formation for s and $C_{V\text{tr},s}$ is the specific (per mass unit) translational-rotational heat capacity at a constant volume.

The vibrational energy is intrinsic only for two-atom and multi-atom molecules; it is equal to zero for atoms.

Here, in contrast to the flow with lower velocities, the hypersonic flow is described by a larger number of parameters. For an incompressible flow we have four main parameters (the components of the velocity vector and pressure); for a compressible flow at $M < 6$ we have five parameters (the components of the velocity vector, temperature, and pressure/density) and for a hypersonic flow we have more than eight depending on the chemical composition of the media (the components of the velocity vector, total energy, vibrational energy, and the concentrations of the components).

Therefore, the set of equations of the stability theory that are derived with the use of decomposition (1) becomes more complicated: equations for disturbances, the vibration temperature, and the densities of the components are added. As a result, the number of parameters that influence the flow stability and the position of the laminar–turbulent transition becomes larger.

In a linear approximation the set of stability equations for a flat layer can be written as follows [24]:

$$\left(A\frac{d^2}{dy^2} + B\frac{d}{dy} + C\right)\hat{\mathbf{q}} = 0.$$

Here $\hat{\mathbf{q}}(y) = [\hat{\rho}, \hat{u}(y), \hat{v}(y), \hat{w}(y), \hat{T}, \hat{T}_{v1} \ldots \hat{T}_{vm}, \hat{C}_1(y) \ldots \hat{C}_{N_C}(y)]^T$ is the vector of the unknown values (form functions); m is the number of molecular vibrational modes; and A, B, C are complex matrixes with a dimensionality minimum of $N_C + m + 5$ (if the mixture can be characterized only by the vibration temperature).

The set of equations is solved jointly with the equations for the averaged values. Methods for solving equations for averaged characteristics at high velocities were discussed in detail in [25, 26] (for structured meshes) and in [27] (for unstructured ones).

The described approach makes it possible to investigate hypersonic laminar flow stability with respect to the receptivity to unstable waves and to different factors that influence the laminar–turbulent transition.

In particular, by using the stability-theory equations using the definition described above it is possible to explain the effect of flow stabilization in case of carbon-dioxide gas injection into the boundary layer.

4. FACTORS THAT INFLUENCE THE LAMINAR–TURBULENT TRANSITION

Since the experimentsof Reynolds on the stability of a laminar flow in a circular pipe, a large amount of experimental and theoretical experience has been accumulated in analyzing different factors that influ-

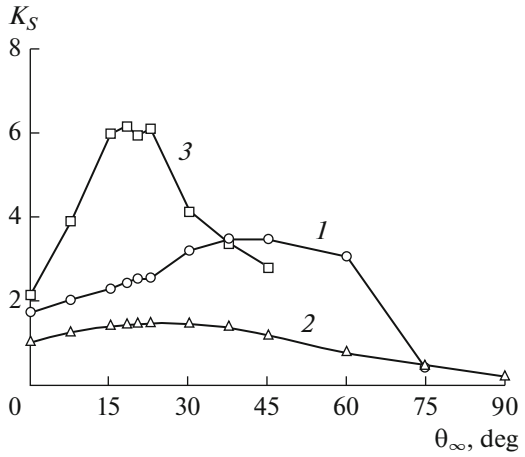

Fig. 5. The coefficient of the intensification of different modes in a high-velocity boundary layer during the impact of external acoustic vibrations as a function of their incident angle [32]: *1*, I stable mode, *2*, II Mack mode, *3*, II stable mode.

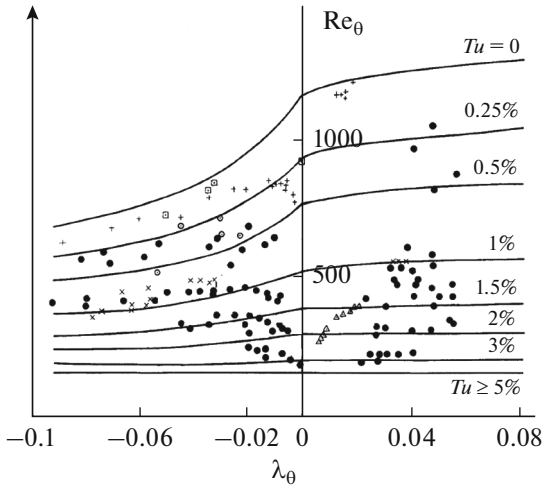

Fig. 6. The relationship between the transition Reynolds number and the pressure gradient at different turbulization levels of the external flow *Tu* [33]: the points are the experimental data; the lines are the empirical relationships.

ence the laminar–turbulent transition. Incompressible and compressible flows; subsonic, supersonic, and hypersonic boundary layers; and flows around bodies with different shapes have been studied.

Factors that influence the prevailing (having the largest amplification rate) mechanism of stability loss and laminar boundary layer destruction can be separated into external and internal ones. The external factors are as follows: pressure gradients, acoustic wave impacts, and parameters of the incoming flow such as its velocity and turbulence intensity (i.e., external factors). The internal factors are as follows: surface roughness and porosity, heat-mass exchange with the surface, and several other factors.

Here, we examine the most important factors that influence the laminar–turbulent transition in a boundary layer.

4.1. Acoustic Impacts

When we investigate low-turbulent flows at ground conditions (in a wind tunnel) typical for the flight conditions of a high-velocity vehicle, the main external impact that causes disturbances in a laminar boundary layer are acoustic waves that occur in the incoming flow. When an acoustic wave arrives at a plate, disturbances are generated in the boundary layer. The largest impact causes a wave that moves to the front edge, which can be due to the small thickness of the boundary layer in this area [28, 29]. When the incoming acoustic wave interacts with a separated wave, three types of disturbances occur in the boundary layer: vortex, acoustic, and entropy waves. It is necessary to note that in the incoming flow two waves occur simultaneously: slow and fast waves with phase velocities of $1 - 1/M_\infty$ and $1 + 1/M_\infty$, respectively. One wave spreads along the flow, the second wave spreads in the opposite direction, but since the flow is supersonic, both waves move in the flow direction. In this case the coefficient of receptivity to the slow acoustic wave is higher than to the fast one [28]. Waves reflected from the boundary layer edge and wall interact each other and may (if the phase velocities are synchronized) resonate with stable wave modes that exist in the flow; as a result, the vibration amplitude of the latter increase and instability waves of the first or second mode occur [30, 31].

It has been found that boundary-layer receptivity to an acoustic wave depends on the incident angle to the wall. It has been shown that there is a relationship between the receptivity factor and the incident angle of the wave (Fig. 5). The intensification coefficient K_S is the ratio between the maximal amplitude of the pressure disturbance and the pressure in the incoming flow.

Boundary-layer behavior near a cone surface caused by an acoustic wave is similar to the boundary layer behavior at a flat plate. Acoustic waves influence stability and transport disturbances most efficiently if they are incident to the cone vertex.

4.2. Pressure Gradient

The effect of a pressure gradient has been studied properly for the case of the instability of the first mode. Experiments are in good agreement with theoretical predictions, where a positive gradient causes a destabilizing effect and a negative gradient causes a stabilizing one. A detailed review of experimental investigations related to this phenomenon was presented in [33].

Figure 6 depicts the relationship between the transition Reynolds number and pressure gradient at different levels of turbulization of the external flow for

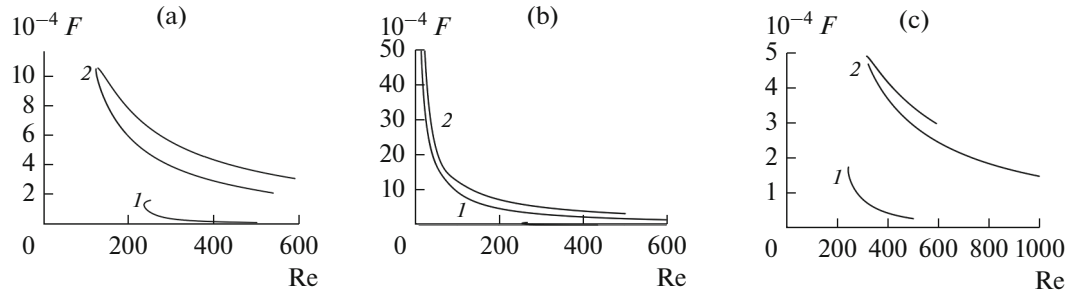

Fig. 7. Curves of the neutral stability of the first (*1*) and second (*2*) modes at M = 5.35 and at different pressure gradients: (a) $\lambda_s = 0$; (b) –0.01, (c) 0.01.

low flow velocities. In this case the pressure gradient can be written as follows:

$$\lambda_\theta = \frac{\theta^2}{\nu}\frac{dU_\infty}{dx}.$$

The calculations presented in [34] give an interesting picture of how the pressure gradient influences the stabilization process of instability modes. In [34] the following parameter characterizing the pressure gradient in a flow was used (in the authors' terminology it is called the gradient parameter):

$$\lambda_s = -\frac{s}{\rho_e u_e}\frac{dp}{ds}.$$

For moderate Mach numbers (M ~ 2), i.e., in the area where the first instability mode is dominant, the effect of a pressure gradient in the boundary layer is similar to the low-velocity case (a positive pressure gradient causes a destabilizing effect, while a negative pressure gradient causes a stabilizing effect).

For high Mach numbers (M ~ 5) and small gradient parameters ($|\lambda_s| < 0.015$) we see a reverse relationship between the critical Reynolds number and pressure gradient for the first mode disturbance, i.e., the negative pressure gradient destabilizes the first mode, while a positive pressure gradient stabilizes it [34]. At $|\lambda_s| > 0.015$ the reversal of the relationship does not occur.

The effect of a pressure gradient on the second mode is classical, i.e., a negative gradient stabilizes the second mode, while a positive pressure gradient strongly destabilizes it. The total effect of a pressure gradient to a high-velocity flow with a tendency to second mode domination for a small gradient parameter is such that for a positive pressure gradient the boundary layer stability is determined only by the second mode, while for a negative pressure gradient it is determined by the first one (Figs. 7, 8).

For high Mach numbers of the incoming flow and gradient parameters $|\lambda_s| > 0.015$ the effect of the first mode is dominant, the second mode is unstable, and the resulting effect of the pressure gradient to the flow is classical since the reversal effect disappears.

Unfortunately we were not able to find data similar to the results presented in Fig. 6 for a high-velocity flow.

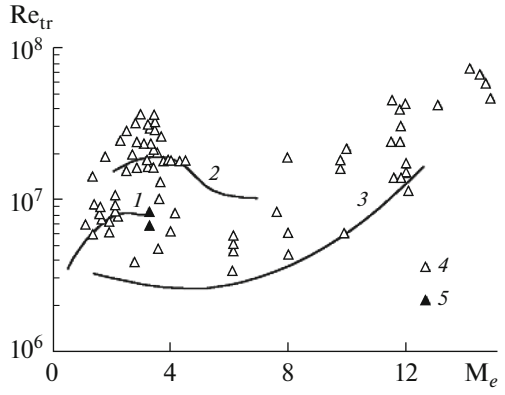

Fig. 8. The relationship between the transition Reynolds number and the Mach number at the edge of the boundary layer: *1*, *2*, calculations according to the e^N ($N = 10$) method for adiabatic and cooling walls, respectively; *3*, experimental data for ordinary wind tunnels; *4*, the results of flight experiments; *5*, experimental data for low-noise wind tunnels.

4.3. Mach Number

The Mach number of the incoming flow can influence the position of the laminar–turbulent transition. If the Mach number increases the turbulence moves downflow [35].

Figure 8 depicts the respective experimental and calculated results for flow around a cone.

4.4. Heat Exchange on the Surface of a Body with Flow Around It

The effects that occur during heat exchange on a surface with flow around it are important. In practice the most interesting situation is the case of flow cooling ($T_w/T_r < 1$).

Using stability theory it is shown that first-mode disturbances are stabilized by flow cooling, while second-mode disturbances are destabilized. Here, in flows where the first mode disturbances are determi-

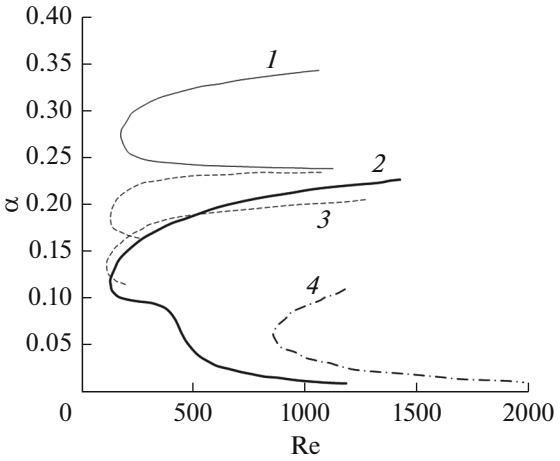

Fig. 9. The wall cooling effect on the neutral stability curve at M = 5.8; 2D disturbances, $T_\infty = 125$ K according to [36]: *1*, $T_w/T_r = 0.05$, *2*, adiabatic wall; *3*, 0.25, *4*, 0.65.

native in the mechanism of boundary layer destruction, the flow cooling stabilizes the flow and closes the laminar–turbulent transition, while in flows with a higher velocity, where the second instability mode is prevalent, flow cooling destabilizing the flow and accelerates the transition to turbulence.

Figure 9 depicts the neutral curves for the flow in a 2D boundary layer for a flat plate when the wall is cooled.

4.5. Gas Injection into the Boundary Layer

Different investigations (see, for example, [21, 37, 38]) have shown that gas injection into a boundary layer can greatly influence the laminar–turbulence transition in the boundary layer.

The qualitative character of this effect depends on the chemical composition of the injected gas and the injection parameters.

The physical mechanisms of this effect were investigated numerically using the Navier–Stokes equations and stability theory.

It is possible to separate the following factors due to which the gas injection can influence laminar–turbulent transition: growth of the boundary layer thickness and effects connected with the chemical composition of the injected gas.

According to the data presented in [39] (without considering the chemical reactions and molecular vibrations) gas injection increases the boundary layer thickness; as a result it increases the wavelength (decreases amplitude) of the disturbance mode and deforms the velocity vector of the averaged flow. As a result it causes area displacement from the wall with large frictional stresses and the stabilizing effect of viscosity decreases. Here, in terms of hydrodynamics the gas injection into boundary layer causes a destabilizing effect and accelerates the laminar–turbulent transition.

On the other hand, in some cases gas injection can stabilize the boundary layer. This concerns physical and chemical processes connected with chemical reactions and molecular vibrations. Usually these processes take place in high-enthalpy flows.

In particular, it has been found that carbon-dioxide gas injection into a high-velocity air flow stabilizes the boundary layer by decreasing the disturbance factor N and by increasing the transition Reynolds number [40]. It has also been shown that if other gases are injected (nitrogen, argon, and air), we do not observe the same effect [41]. Upon analyzing this phenomenon it has been found that the effect caused by carbon dioxide gas is connected with the vibration-relaxation properties of the CO_2 molecule and with the processes of energy redistribution between the translational and vibrational molecular modes in the boundary layer.

Qualitatively, the effect of the injection of carbon dioxide gas depends on the flow rate at which this gas is injected into the boundary layer; it is characterized by injection parameter

$$f_w = \frac{\sqrt{2\,\mathrm{Re}_x}\rho_w u_e}{\rho_\infty u_\infty}.$$

Since (as mentioned above) gas injection into the boundary layer destabilizes it, there is a definite boundary value of the f_{w0} parameter. If $f_w < f_{w0}$, the molecular-relaxation effects of gas injection prevail and injection of carbon dioxide gas stabilizes the boundary layer; if $f_w > f_{w0}$, the hydrodynamic effects prevail and gas injection destabilizes the boundary layer.

Figure 10 shows the calculated relationship between the point of the laminar–turbulent transition on the cone and the injection parameter.

The effects of argon and nitrogen injection are practically the same. It is seen that for the carbon dioxide gas there is an optimal injection parameter at which the stabilizing effect is maximal.

4.6. Surface State

The surface state greatly influences the boundary-layer stability.

The experiments and the simulation results show that both single obstacles and distributed roughness can cause waves of instability. The main parameters that influence the wave type and the intensity of its growth are the ratio between the obstacle height and boundary-layer thickness and the shape of the obstacle.

As an example, it was found that the largest destabilizing effect is seen if the obstacle height is greater than half of the boundary-layer thickness.

In general, this problem has been investigated insufficiently because different roughnesses and

mutual positions can influence boundary-layer stability in different ways.

In addition to roughness, the problem of the surface porosity effect on the laminar–turbulent transition has been studied in detail.

In the experiments in [42–44] it was shown that with respect to a solid impermeable wall a porous coating greatly decreases the growth of disturbance of the second mode, while it somewhat destabilizes the first mode. It has been shown that at hypersonic flight velocities a porous sound-absorbing coating can increase the region of laminar flow.

5. AN ENGINEERING MODEL OF THE LAMINAR–TURBULENT TRANSITION IN A HIGH-VELOCITY FLOW

Approaches based on stability theory and the e^N method have been developed properly for high-velocity flows but they are of lesser interest from the practical point of view.

Among engineering models, it is possible to distinguish only [45–50]. However, this field is promising due to its simplicity of implementation and the wide application of automated software for computation of hydrodynamics, in which it is practically impossible to use stability theory methods in contrast to engineering methods whose essence is to solve additional semi-empirical transport equations.

In these works, the intermittency concept is used, but there is a difference between them: models [45–49] are differential and model [50] is algebraic and is based on the Cebici–Smith equations.

If we compare these models, we see that models of the [45–49] type are universal, while [50] is more simple.

Here, we present a model of the laminar–turbulent transition, which we developed by generalizing the approach presented in [45–49]. In general, these approaches are similar to the Menter–Langtry approach; we add components that consider the contribution caused by non-turbulent fluctuations.

Formula (8) is used for the effective viscosity. The turbulent viscosity is determined by the corresponding turbulence model; for the non-turbulent viscosity, μ_{nt}, the following relationship is used:

$$\mu_{nt} = C_\mu \rho K \tau_{nt},$$

where $C_\mu = 0.09$ is a constant and K is the kinetic energy of the turbulence.

The characteristic time τ_{nt} consists of two parts:

$$\tau_{nt} = \tau_{nt1} + \tau_{nt2},$$

where τ_{nt1}, τ_{nt2} are the characteristic times of the first and second mode of the disturbances, respectively. These are determined as follows:

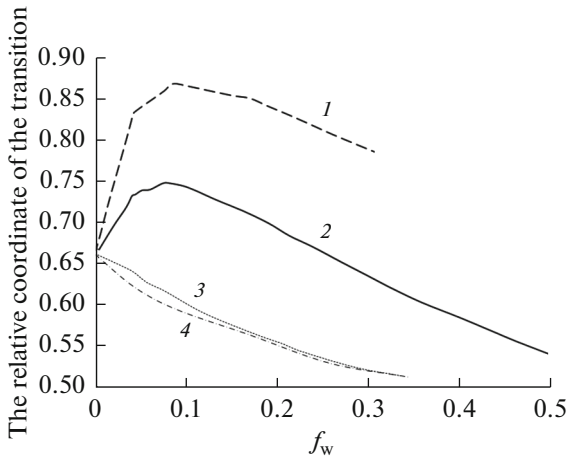

Fig. 10. The relationship between the point of the laminar–turbulent transition and the injection parameters for different gases: *1*, heated CO_2, *2*, CO_2, *3*, Ar, *4*, N_2.

$$\tau_{nt1} = \frac{C_2 \varsigma_{\text{eff}}^{1.5}}{\left[(2E_u)^{0.5} \nu\right]^{0.5}},$$

$$\tau_{nt2} = \frac{C_3 2 \varsigma_{\text{eff}}}{U_P}.$$

Here, ς_{eff} is the effective length scale of the turbulence [48, 49], ν is the coefficient of kinetic viscosity, $E_u = 0.5|U_e|^2$ is the kinetic energy of the external flow, and U_P is the phase velocity for the second mode. This can be estimated as follows [45, 46]

$$U_P = 0.94 U_e,$$

where U_e is the external flow velocity.

The following transport equation is used for determining the intermittency factor [48, 49]

$$\frac{\partial}{\partial t}(\rho\gamma) + \frac{\partial}{\partial x_k}(\rho u_k \gamma) = \frac{\partial}{\partial x_k}\left[\left(\mu + \frac{\mu_{\text{eff}}}{\sigma_\gamma}\right)\frac{\partial \gamma}{\partial x_k}\right] + P_\gamma(F_{\text{onset}}) - \varepsilon_\gamma,$$

$$P_\gamma(F_{\text{onset}}) = P_\gamma = C_4 \rho F_{\text{onset}} [-\ln(1-\gamma)]^{0.5} \left(1 + C_5 \sqrt{\frac{K}{2E_u}}\right) \frac{d}{\nu} |\nabla \tilde{E}_u|,$$

$$\varepsilon_\gamma = \gamma P_\gamma,$$

$$F_{\text{onset}} = 1 - \exp\left(-C_6 \frac{\varsigma_{\text{eff}} K^{0.5} |\nabla K|}{\nu |\nabla E_u|}\right),$$

where d is the distance from the wall.

This equation is solved according to the recommendations presented in [45–49] with zero initial and boundary conditions at the inlet of the computational domain.

Table 1. Experimental parameters [51]

Test	6911	6909, 6910	6912, 6913	6926
M	6.3	6.2	6.1	5.5
Flow velocity, m/s	2980	3210	3370	4330
Static pressure, kPa	2.8	5.4	12.1	9.4
Static temperature, K	570	690	800	1560
Unit Reynolds number Re, 10^6 m^{-1}	1.7	2.6	4.9	1.6

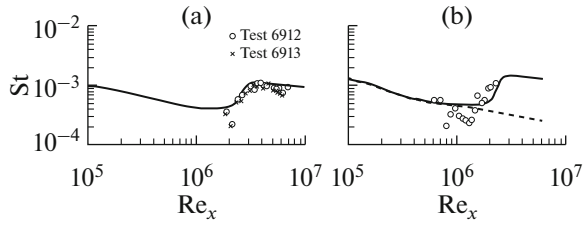

Fig. 11. The Stanton-number distribution along a plate for modes 6912 and 6913 (a) 6926 (b): experimental points [51], solid line, the results of calculations; dashed line, laminar flow calculations (without considering the laminar–turbulent transition).

The following constants are used [48, 49]:

C_μ	C_1	C_2	C_3	C_4	C_5	C_6	σ_γ
0.09	0.7	0.35	0.005	8×10^{-5}	0.07	1.2	1.0

This is a phenomenological model; it does not consider the concrete mechanisms of the transition. The generation structure and constants for the model were obtained in [45–49]. In this paper we generalize and use the approaches that were developed in [45–49].

To verify the model, the calculation results are compared with the experimental data presented in [51], in which the hypersonic laminar–turbulent transition is examined for the plate under conditions presented in Table 1.

Some computation results for the Stanton number, St, are presented in Fig. 11.

It is seen that the model is in good agreement with the experimental data.

CONCLUSIONS

The laminar–turbulent transition in a boundary layer is a complicated hydrodynamic phenomenon that depends on a large number of factors.

A large volume of theoretical and experimental data on the regularities of this phenomenon has been accumulated. Factors that impact the laminar–turbulent transition have also been studied. The problem of systematizing and generalizing the accumulated material is of interest for further work.

In the present work we perform a brief review of the existing procedures for predicting the laminar–turbulent transition and the factors that influence this process.

There are two different approaches for simulating and analyzing the boundary-layer behavior during a laminar–turbulent transition.

In the classical approach the boundary layer is examined as a certain system that transforms external disturbing signals. The aim of this approach is to determine the physical mechanisms that are responsible for the intemittency and transition.

The engineering approach is based on CFD methods where additional semi-empirical transport equations are introduced artificially for characteristics that determine the state of the boundary layer (for example, intermittency). The aim of this approach is to determine the area of the laminar–turbulent transition using computer aided engineering (computational fluid dynamics) software without a detailed analysis of transition mechanisms.

Unfortunately, these approaches are developing independently. Both approaches have advantages and disadvantages, which should be overcome.

In this work we presented an engineering model of the laminar–turbulent transition developed by using the intermittency concept and time scale values typical for different disturbance modes.

Finally, when designing modern high-velocity flying vehicles it is necessary to make a complex examination of the phenomenon of the laminar–turbulent transition by considering different factors that can influence the flow-around conditions.

This problem can be solved only by using theoretical and engineering methods with a large volume of experimental data.

REFERENCES

1. Tarasevich, S.E., Zlobin, A.V., and Yakovlev, A.B., *High Temp.*, 2015, vol. 53, no. 6, p. 908.
2. Kachanov, Y.S., *Annu. Rev. Fluid Mech.*, 1994, vol. 26, p. 411.
3. Morkovin, M.V., Critical evaluation of transition from laminar to turbulent shear layer with emphasis of hypersonically travelling bodies, FFDLTech. Rep. 68-1-49, 1968.
4. Mack, L.M., *AIAA J.*, 1975, vol. 13, no. 3, p. 278.
5. White, E.B., Saric, W.S., Gladden, R.D., and Gabet, P.M., Stages of swept transition, *AIAA Pap.* 2001-0271, 2001.
6. Jie Ren, Song Fu, and Jianxin Liu, in *Proc. 44th AIAA Fluid Dynamics Conf.*, 2014.
7. Morkovin, M.V., On the many faces of transition, in *Viscous Drag Reduction*, Wells, C.S., Ed., London: Plenum, 1969, p. 1.
8. Herbert, T., *Annu. Rev. Fluid Mech.*, 1997, no. 29, p. 245.
9. Schmid, P.J., et al., *Theor. Comput. Fluid Dyn.*, 1993, vol. 4, no. 5, p. 227.

10. Belov, I.A. and Isaev, S.A., *Modelirovanie turbulentnykh techenii* (Simulation of Turbulent Flows), St. Petersburg: Balt. Gos. Tekh. Univ., 2001.
11. Dhawan, S. and Narasimha, R., *J. Fluid Mech.*, 1958, no. 3, p. 418.
12. Menter, F.R., Langtry, R.B., Likki, S.R., Suzen, Y.B., Huang, P.G., and Völker, S., in *Proc. ASME TURBO EXPO 2004*, Vienna, 2004, ASME-GT2004-53452.
13. Menter, F.R., Esch, T., and Kubacki, S., in *Proc. 5th Int. Symposium on Turbulence Modeling and Measurements*, Spain, 2002.
14. Langtry, R.B. and Menter, F., Transition modeling for general CFD applications in aeronautics, *AIAA Pap.* 2005-522, 2005.
15. Menter, F.R., Langtry, R., and Völker, S., *Flow, Turbul. Combust.*, 2006, vol. 77, nos. 1–4, p. 277.
16. Langtry, R.B. and Menter, F.R., *AIAA J.*, 2009, vol. 47, no. 12, p. 2894.
17. Walters, D.K. and Cokljat, D., *J. Fluids Eng.*, 2008, vol. 130, no. 12, p. 121401.
18. Özgen, S. and Kırcalı, S.A., *Theor. Comput. Fluid Dyn.*, 2008, vol. 22, p. 1.
19. Fedorov, A.V., *Annu. Rev. Fluid Mech.*, 2011, vol. 43, p. 79.
20. Demetriades, A., Hypersonic viscous flow over a slender cone. Part III: Laminar instability and transition, *AIAA Pap.* 74-535, 1974.
21. Malik, M.R., *AIAA J.*, 1989, vol. 27, no. 11, p. 1487.
22. Surzhikov, S.T., *High Temp.*, 2016, vol. 54, no. 2, p. 235.
23. Bykov, L.V., Molchanov, A.M., Shcherbakov, M.A., and Yanyshev, D.S., *Vychislitel'naya mekhanika sploshnykh sred v zadachakh aviatsionnoi i kosmicheskoi tekhniki* (Computational Mechanics of Continuous Media in the Problems of Aviation and Space Technology), Moscow: Lenand, 2015.
24. Hudson, M.L. and Chokani, N., *AIAA J.*, 1997, vol. 35, no. 6, p. 958.
25. Molchanov, A.M., *Matematicheskoe modelirovanie zadach gazodinamiki i teplomassoobmena* (Mathematical Simulation of Gas Dynamics and Heat and Mass Transfer Problems), Moscow: Mosk. Aviats. Inst., 2013.
26. Egorov, I.V., Pal'chekovskaya, N.V., and Shvedchenko, V.V., *High Temp.*, 2015, vol. 53, no. 5, p. 677.
27. Zheleznyakova, A.L. and Surzhikov, S.T., *High Temp.*, 2014, vol. 52, no. 2, p. 271.
28. Yanbao Ma and Xiaolin Zhong, *J. Fluid Mech.*, 2003, vol. 488, p. 31.
29. Maslov, A.A., Shiplyuk, A.N., Sidorenko, A.A., and Arnal, D., *J. Fluid Mech.*, 2001, vol. 426, p. 73.
30. Balakumar, P., Transition in a supersonic boundary layer due to acoustic disturbances, *AIAA Pap.* 2005-0096, 2005.
31. Ghaffari, S., Marxen, O., Iaccarino, G., and Shaqfeh, E.S.G., Numerical simulations of hypersonic boundary-layer instability with wall blowing, *AIAA Pap.* 2010-706, 2010.
32. Yanbao Ma and Xiaolin Zhong, *J. Fluid Mech.*, 2003, vol. 488, p. 79.
33. Abu-Ghannam, B.J. and Shaw, R., *J. Mech. Eng. Sci.*, 1980, vol. 22, no. 5, p. 213.
34. Gaponov, S.A. and Terekhova, N.M., *Vest. Novosib. Gos. Univ.*, 2013, vol. 13, no. 4, p. 64.
35. Stetson, K.F., Hypersonic boundary layer transition experiments, Tech. rep. AFWAL-TR-80-3062, 1980.
36. Reshotko, E., *Annu. Rev. Fluid Mech.*, 1976, no. 8, p. 311.
37. Schneider, S.P., Hypersonic boundary-layer transition with ablation and blowing, *AIAA Pap.* 2008-3730, 2008.
38. Johnson, H.B., Gronvall, J.E., and Candler, G.V., Reacting hypersonic boundary layer stability with blowing and suction, *AIAA Pap.* 2009-938, 2009.
39. Ghaffari, S., Marxen, O., Iaccarino, G., and Shaqfeh, E.S.G., in *Proc. 48th AIAA Aerospace Science Meeting Including the New Horizons Forum and Aerospace Exposition,* 2010.
40. Leyva, I.A., Laurence, S., Beierholm, A.K.-W., Hornung, H.G., Wagnild, R., and Candler, G., Transition delay in hypervelocity boundary layers by means of CO_2/acoustic instability interactions, *AIAA Pap.* 2009-1287, 2009.
41. Wagnild, R., High enthalpy effects on two boundary layer disturbances in supersonic and hypersonic flow, *PhD Thesis*, Minneapolis: University of Minnesota, 2012.
42. Rasheed, A., Hornung, H.G., Fedorov, A.V., and Malmuth, N.D., *AIAA J.*, 2002, vol. 40, no. 3, p. 481.
43. Fedorov, A., Shiplyuk, A., Maslov, A., Burov, E., and Malmuth, N., *J. Fluid Mech.*, 2003, vol. 479, p. 99.
44. Gaponov, S.A. and Terekhova, N.M., *J. Appl. Mech. Tech. Phys.*, 2009, vol. 50, no. 5, p. 733.
45. Papp, J.L., Kenzakowski, D.C., and Dash, S.M., Extensions of a rapid engineering approach to modeling hypersonic laminar to turbulent transitional flows, *AIAA Pap.* 2005-892, 2005.
46. Papp, J.L. and Dash, S.M., A rapid engineering approach to modeling hypersonic laminar to turbulent transitional flows for 2D and 3D geometries, *AIAA Pap.* 2008-2600, 2008.
47. Papp, J.L. and Dash, S.M., Modeling hypersonic laminar to turbulent transitional flows for 3D geometries using a two-equation onset and intermittency transport models, *AIAA Pap.* 2012-0449, 2012.
48. Wang, L. and Song Fu, *Sci. China, Ser. G: Phys., Mech. Astron.*, 2009, vol. 52, no. 5, p. 768.
49. Wang, L. and Song Fu, *Flow, Turbul. Combust.*, 2011, vol. 87, p. 165.
50. Gorskii, V.V. and Pugach, M.A., *High Temp.*, 2015, vol. 53, no. 2, p. 223.
51. Mee, D.J., Boundary layer transition measurements in hypervelocity flows in a shock tunnel, *AIAA Pap.* 2001-0208, 2001.

Translated by Yu.V. Zikeeva